Ultra High Speed Coherent Optical Communication Using Digital Signal Processing Techniques Along With Advanced Modulation System

Md. Siam Uddin[1], Md. Amir Hamja[2]
Dept. of EEE
[1, 2]University of Dhaka (Mymensingh Engineering College)
Mymensingh, Bangladesh
siam@eee.mec.ac.bd

***Abstract*— Recent coherent optical communication systems address modulation and detection techniques for high spectral efficiency and robustness against transmission impairments. This paper demonstrates the generation and transmission of beyond 400Gb/s transmission system over the standard 50GHz ITU-T grid at a net spectral efficiency of 8.4b/s/Hz. Coherent detection employing QAM modulation formats along with DSP algorithm have become one of the most promising technologies for next generation high speed transmission systems due to the high power and spectral efficiencies. This paper shows that, the use of near ideal Nyquist pulse shaping, spectrally-efficient high-order modulation format, and distributed Raman amplification, coherent equalization may enable us to operate future 400G systems over the standard 50GHz-grid optical network.**

Keywords—Wave length division multiplexing (WDM); coherent detection; digital signal processing (DSP); QAM; Nyquist pulse.

I. INTRODUCTION

In order to cope with the increasing global information exchange it's becoming crucial to transmit information over longer distance. A solution to this issue is optical fibers that are already used for most of the voice and data traffic all over the world. Optical fibers are exceptionally advantageous for long-haul communication systems.

The reason behind it, when light propagates through an optical fiber it suffers from less attenuation than the case of an electrical cable. Moreover it's possible to transmit several channels, at different wavelength, on the same medium using wave length division multiplexing (WDM). This enables to reach a capacity system of several Tb/s. Recently, digital coherent optical communication has become the main technology for optical transport networks [1]. Moreover, digital signal processing is under consideration as a promising technique for optical signal modulation, fiber transmission, signal detection and dispersion compensation. There are different reasons why the utilization of coherent detection associated digital signal processing can be very advantageous. Firstly, coherent detection is a promising technology to increase optical receiver sensitivity, permitting a greater span loss to be tolerated. Secondly, coherent detection enables supporting of more spectrally efficient modulation formats such as quadrature phase shift keying (QPSK) and quadrature amplitude modulation (QAM). And finally, instead of implementing costly physical impairments compensation links, coherent detection allows digital signal processing for compensation of transmission impairments such as CD, polarization mode dispersion (PMD), signal carrier offset, spectrum narrowing etc. Furthermore, next generation optical transmission systems require adaptive fitting for time varying transmission impairments such as channel spectrum narrowing and random phase noise. Digital signal processing is a powerful solution for future adaptive optical transmission links.

Recently, 400G transmission over the standard 50GHz WDM grid has been demonstrated by using PDM-32QAM based modulation [2-4]. In [3], 8×450Gb/s WDM signals over 400km of ULAF fiber and passing through one 50GHz-grid WSS-based reconfigurable add/drop multiplexer (ROADM) has been demonstrated at a net spectral efficiency (SE) of 8b/s/Hz. This is the first experimental demonstration for 400G WDM system over the standard 50GHz-grid optical network.

II. THEORETICAL OVERVIEW OF COHERENT DETECTION

In coherent detection systems, a complex modulated signal, whose information lies not only on its amplitude but phase as well, can be written as:

$$E_S(t) = A_S(t)\exp[i(\omega_S t + \phi_S)] \quad (1)$$

Where ω_S and ϕ_S are the signal's carrier frequency and time dependent phase variable, and $A_S(t)$ is the amplitude component of the signal. The optical field associated with the local oscillator (LO) can be written as:

$$E_{LO}(t) = A_{LO}(t)\exp[i(\omega_{LO} t + \phi_{LO})] \quad (2)$$

Where ω_{LO}, $A_{LO}(t)$ and ϕ_{LO} are respectively the carrier frequency, amplitude and time dependent phase variable of the

LO. The scalar notation is used for both $E_S(t)$ and $E_{LO}(t)$ due to assuming that two fields are identically polarized [5].

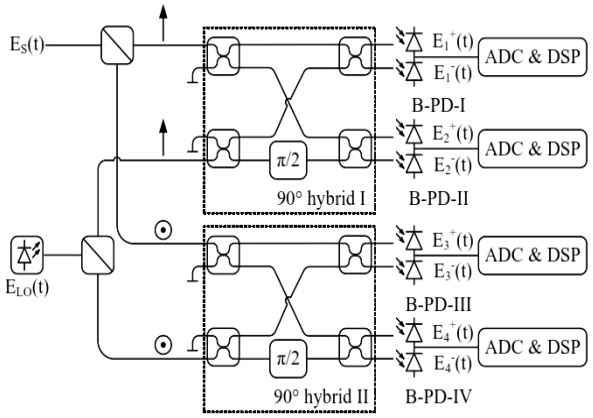

Fig. 1. Dual polarization coherent detection with balanced PD.

There are different coherent detection schematics to cope with the coherent detection technique denoted as single coherent detection with single photodiode (PD), single coherent detection with balanced-photodiode (B-PD), quadrature coherent detection with 90°-hybrid and dual polarization coherent detection.

International telecommunication union (ITU) defined criteria as, channel spacing of 100 Gb/s optical communication systems is assigned to be 50 GHz. In order to fulfill such bandwidth requirements, dual polarization coherent detection with balanced PD will better option. As it is explored by several researches [6-7], polarization diversity is under consideration as the third degree of modulation freedom. As two of in-phase and quadrature modulation formats are capable for any level complex modulation then dual polarization will further double the capacity of transmission systems [8]. Recently, single-channel bit-rates beyond 100-Gb/s have been demonstrated by using both single-carrier (up to 448-Gb/s) [9] and multi-carrier based high-order coherent modulation formats (up to 448-Gb/s [10,11] and 1.2-Tb/s [12]). For WDM transmission, 50GHz-spaced, 10x224Gb/s over 12x100km at a SE of 4b/s/Hz [13], 10x456Gb/s in 70GHz channel spacing over 8x100km at SE=6.1bit/s/Hz [13], and 100GHz-spaced, 3x485Gb/s over 48x100km at SE=4b/s/Hz [14] have been demonstrated by using PDM-16QAM based modulation, digital coherent detection, distributed Raman amplification as well as new ultra-large area fiber (ULAF).

III. TECHNICAL DESCRIPTION OF DSP

The common configuration of optical coherent receiver associated with DSP algorithms is shown in Fig. 3. Coherent detection with DSP algorithms can take advantage from continuously increasing electrical processing speed. Consequently, it is efficient and simple to implement optical signal processing in digital domain. Four main functions are performed in digital domain: 1) Dispersion compensation, 2) Clock recovery, 3) Polarization de-multiplexing, and 4) Carrier phase estimation.

A. Dispersion Compensation

The frequency response for an all-pass filter to compensate fiber CD can be expressed as in the absence of fiber nonlinearity:

$$G(z,\omega)=\exp[-jD\frac{\lambda^2}{2\pi c}\frac{\omega^2}{2}z+jS\left(\frac{\lambda^2}{2\pi c}\right)^2\frac{\omega^3}{6}z] \quad (3)$$

Where D is the dispersion coefficient, S is the dispersion slop, ω is the angular frequency, λ is the light wavelength, c is the light velocity, and z is the fiber length. In order to compensate for the dispersion, the output field is multiplied to the inverse of the channel transfer function (FIR filter) [15]. After CD compensation at frequency domain, IFFT inverts the sequence back to the time domain.

B. Clock Recovery

In general, any sampling clock errors significantly reduce system BER performance. Therefore clock recovery DSP algorithm is demanded to determine the suitable sampling clock.

The clock recovery DSP algorithm implemented in this paper is known as Gardner algorithm [16], which is widely used in the field of wireless communication systems. Structure of Gardner clock recovery is shown in Fig. 2. The numerically controlled oscillator (NCO) is driven by outputs from Gardner time error detector $e_x(n)$ and $e_y(n)$, which are defined in equation 4 and equation 5.

$$e_x(n)=X_I(n)[X_I(n+1)-X_I(n-1)]+X_Q(n)[X_Q(n+1)-X_Q(n-1)] \quad (4)$$

$$e_y(n)=Y_I(n)[Y_I(n+1)-Y_I(n-1)]+Y_Q(n)[Y_Q(n+1)-Y_Q(n-1)] \quad (5)$$

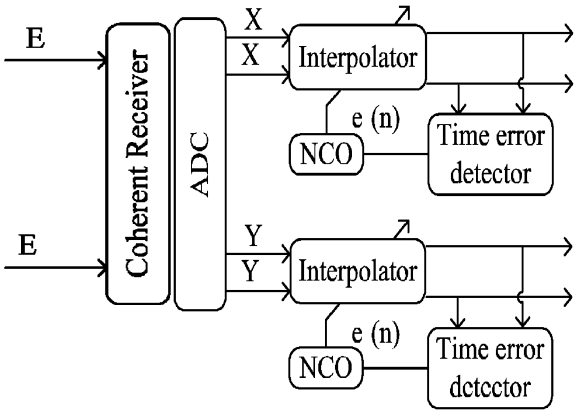

Fig. 2. Structure of Gardner clock recovery DSP algorithm.

Where n-th element of time error represents difference between two adjacent samples from ADC. Sample period is equal to $T_S/2$, where T_S is symbol period of transmitted signal. The implementation of interpolator is used to interpolate adjacent symbols with new sampling clock. The mean purpose of Gardner clock recovery algorithm is to sample the adjacent sequences with the same time difference that $e_x(n)$ and $e_y(n)$ are equal to zero.

C. Polarization Demultiplexing

In order to emulate the cross-talk between the signals carried on two polarizations, Jones matrix is employed, which is given as

$$\begin{pmatrix} \sqrt{\alpha e^{i\delta}} & -\sqrt{1-\alpha} \\ \sqrt{1-\alpha} & \sqrt{\alpha e^{-i\delta}} \end{pmatrix} \tag{6}$$

Where α and δ denote the power splitting ratio and phase difference between two polarizations. Therefore the polarization multiplexed signal at the receiver side after fiber propagation can be presented as [17].

$$\begin{bmatrix} E_x \\ E_y \end{bmatrix} = \begin{pmatrix} \sqrt{\alpha e^{i\delta}} & -\sqrt{1-\alpha} \\ \sqrt{1-\alpha} & \sqrt{\alpha e^{-i\delta}} \end{pmatrix} \begin{bmatrix} E_{in,x} \\ E_{in,y} \end{bmatrix} \tag{7}$$

So if the inverse of Jones matrix is found, polarization de-multiplexing can be performed.

$$\begin{bmatrix} E_X \\ E_Y \end{bmatrix} = \begin{pmatrix} P_{xx} & P_{xy} \\ P_{yx} & P_{yy} \end{pmatrix} \begin{bmatrix} E_x \\ E_y \end{bmatrix} \tag{8}$$

The matrix elements are updated symbol by symbol according to

$$P_{xx}(n+1) = P_{xx}(n) + \mu(1 - |E_x(n)|^2) E_x(n) E_x^*(n) \tag{9}$$

$$P_{xy}(n+1) = P_{xy}(n) + \mu(1 - |E_x(n)|^2) E_x(n) E_y^*(n) \tag{10}$$

μ is the step-size parameter and n is the number of symbols. The P matrix is basically an adaptive FIR filter and we use CMA for blind estimation [18]. The initial values for $P_{xx}(0)$ and $P_{yy}(0)$ are: $P_{xx}(0)$ = [00…010..00];$P_{yy}(0)$ = [00…010..00]; again $P_{xy}(0) = P_{yx}(0)$= [00…000..00]. In this simulation a 3-tap FIR filter, however the order can be changed is chosen.

D. Carrier Phase Estimation

Phase locking in the hardware domain can be replaced by phase estimation in digital domain by DSP [19]. The received QPSK signal can be presented to estimate the phase of the signal in digital domain by

$$E(t) = A \exp\{j[\theta_S(t) + \theta_C(t)]\} \tag{11}$$

The configuration of optical coherent receiver associated with DSP algorithms is shown in Fig. 3.

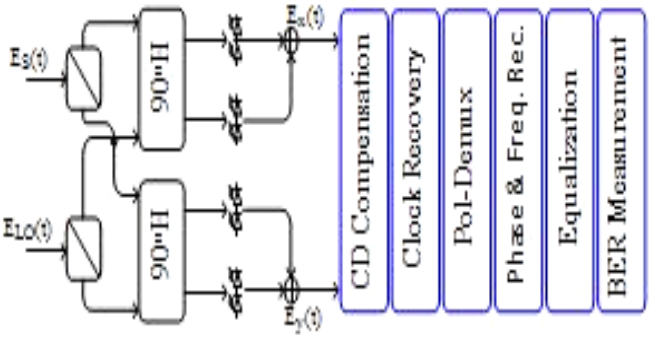

Fig. 3. Configuration of coherent detection with DSP.

In this block diagram, several DSP algorithms are under consideration. CD compensation block is used to compensate for chromatic dispersion. Clock recovery block is implemented to correct digital sampling error which is made by analog to digital converters (ADC). Polarization de-multiplexing is realized by using polarization de-multiplex algorithm. Phase and frequency offset recovery block is employed to correct phase and frequency difference between received signal and Local Oscillator.

IV. 450GB/S PDM-NYQUIST-32-QAM TRANSMITTER

Overcome the limitation of available digital-to-analog (D/A) converter bandwidth, a frequency-locked five-subcarrier generation method has been utilized to create the 450Gb/s per-channel signal [10, 11]. Fig. 4 shows the demonstrated 450Gb/s PDM-Nyquist-32QAM transmitter. The output from a continuous-wave (CW) laser with linewidth ~ 100kHz is split by a 3dB optical coupler (OC). One output is sent to a Mach-Zehnder modulator (MZM-1) driven with a 9.2GHz clock to generate two 18.4GHz-spaced subcarriers per channel (i.e. the two first-order signal components) offset by ±9.2GHz from the original wavelengths. After an erbium-doped fiber amplifier (EDFA) and a 12.5/25GHz interleaver filter (ILF), the original wavelengths and second-order harmonics are suppressed by more than 40dB relative to the first-order components in Fig. 4. The signal is then equally split between two outputs of a polarization beam splitter (PBS) prepared via a polarization controller (PC). The two subcarriers on one PBS output are sent to an IQ modulator (IQ MOD1), driven with a pre-equalized 9Gbaud Nyquist 32-QAM signal with 2^{15}-1 pseudorandom pattern length. The Nyquist pulse shaping has roll-off factor of 0.01, and the digital Nyquist filter has a tap length of 64.

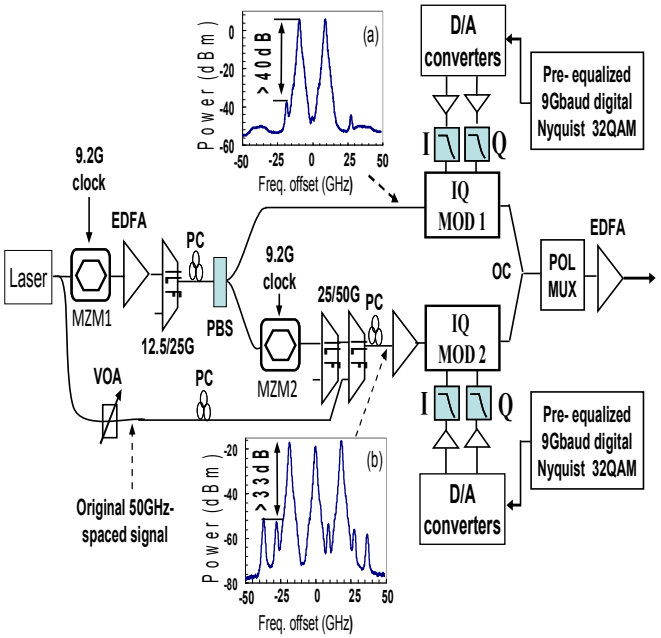

Fig. 4. 450Gb/s PDM-Nyquist-32QAM transmitter. VOA: variable attenuator, PC: polarization controller, PBS: polarization beam splitter.

Fig. 5 shows the Nyquist filter impulse response used in this experiment and the resulting eye diagram of the generated 32QAM baseband signal in one quadrature. Frequency-domain based pre-equalization [12] is used to compensate for the band-limiting effects of the D/A converters, which have 3-dB bandwidths < 5GHz at 10bit resolution and a 24GSa/s sample rate. The measured relative amplitude spectra of the generated 9Gbaud Nyquist 32QAM baseband electrical drive signals (after D/A converters) with and without pre-equalization are shown in Fig. 6. One can see that the filtering effects caused by the D/A converters are effectively compensated by using frequency-domain based digital pre-equalization.

A second Mach-Zehnder modulator (MZM-2) driven with a 9.2GHz clock is placed at the second PBS output to generate first-order signal components at 0GHz and 18.4GHz offsets from the original wavelength. After MZM-2, the signals pass through two 25/50GHz interleavers to suppress the 0GHz signal components and the unwanted harmonics in Fig. 4. The second ILF re-inserts the original CW signal (from the second 3dB OC output), resulting in three 18.4GHz-spaced subcarriers from the original wavelength. These three sub-carriers pass through an IQ modulator (IQ MOD2), driven by a second pre-equalized 9Gbaud Nyquist 32-QAM signal having 2^{15}-1 pseudorandom pattern length and originating from a second D/A converter. Then the sets of two and three 45Gb/s sub-carriers are passively combined and polarization multiplexed with 20ns relative delay, resulting in a 450Gb/s signal that occupies a spectral width of 45.8GHz, sufficiently confined to be placed on the 50GHz ITU grid.

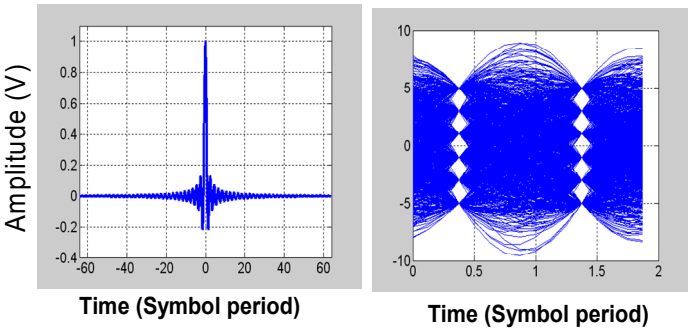

Fig. 5. (a) Interpolated impulse response of the Nyquist filter and (b) the resulting eye diagram of the generated baseband 32QAM signal.

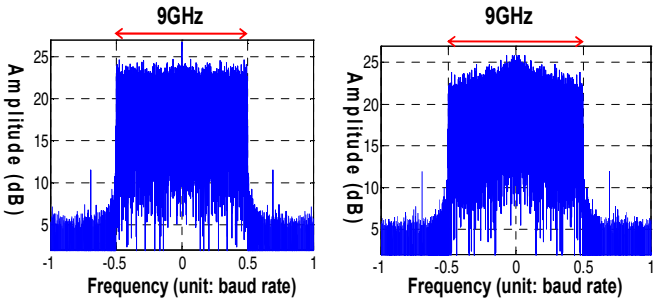

Fig. 6. Measured relative amplitude spectra of 9Gbaud Nyquist 32QAM baseband electrical drive signals (after D/A converter) without pre-equalization (a) and with pre-equalization (b).

V. Result and Discussion

Fig. 7 and Fig. 8 unveil constellation visualizer of X and Y polarization respectively. These results are found from Optisystem runtime package software.

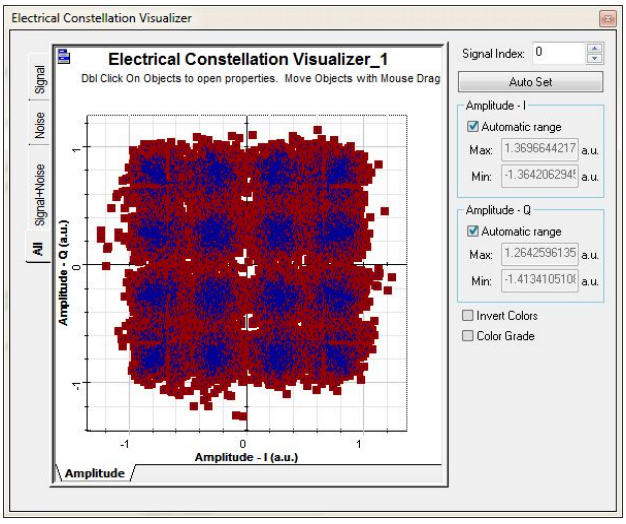

Fig. 7. Constellation visualizer of polarization X.

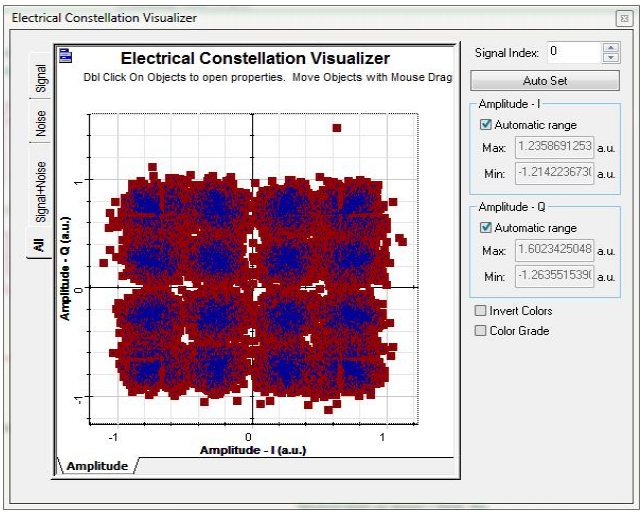

Fig. 8. Constellation visualizer of polarization Y.

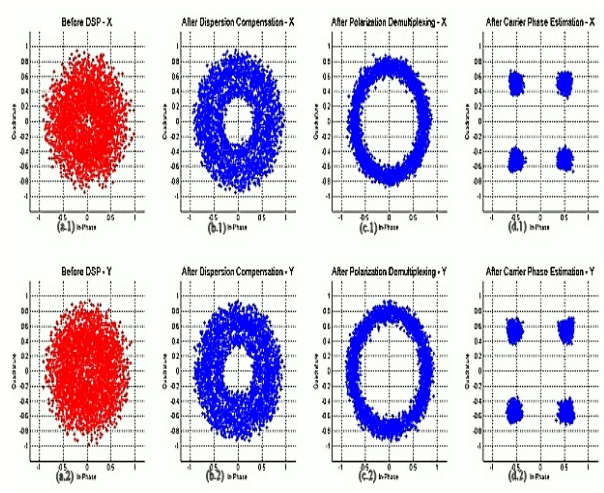

Fig. 9. Matlab implementation of DSP algorithm. (a.1, a.2) Before DSP of X & Y. (b.1, b.2) After dispersion compensation. (c.1, c.2) After polarization demultiplexing. (d.1, d.2) After carrier phase estimation.

These figures emphasize on QAM for ultra-high speed. The algorithms used for digital signal processing are implemented through a Matlab component. By setting the Matlab component to debug mode, the generated electrical constellation diagrams after each step (CD compensation, Polarization De-multiplexing, and Carrier Phase Estimation) are shown here in Fig. 9.

VI. CONCLUSION

According to the recently demonstrated high-SE (8.4b/s/Hz) 400Gb/s per channel WDM signals can be transmitted over the conventional 50GHz ITU-T grid with a transmission reach up to 800km (eight 100km spans) and moreover, passing through one 50GHz grid. These results are accomplished by the use of a spectrally-efficient high-order modulation format, Nyquist-shaped PDM-32QAM, as well as both pre- and post-transmission digital equalization. Low-nonlinearity fiber and low-noise Raman amplification also have been used to address the reduced nonlinear and noise tolerance of the high-order modulation format.

To overcome the bandwidth limitation of the available D/A converters, a frequency-locked five subcarrier generation method with high sideband suppression has used to create the 450Gb/s PDM-Nyquist-32QAM signals. The use of five frequency-locked subcarriers and near ideal Nyquist pulse shaping essentially allows the 450Gb/s spectrum being well confined within the 50GHz channel spacing (occupying a signal spectral width about 45.8GHz). Using multiple subcarriers (with Nyquist pulse shaping) within each channel could enable all-optical sub-wavelength grooming, which may be useful for future 400Gb/s and beyond ultra-high-speed systems.

REFERENCES

[1] Chongjin Xie, "Chromatic dispersion estimation for single-carrier coherent optical communication," IEEE Photonics Technology Letters, vol. 25, no. 10, pp. 992-995, May 2013.

[2] P. J. Winzer, A. H. Gnauck, S. Chandrasekhar, S. Draving, J. Evangelista, and B. Zhu, "Generation and 1,200-km transmission of 448-Gb/s ETDM 56-Gbaud PDM 16-QAM using a single I/Q modulator," ECOC 2010, Torino, Italy, PDP 2.2, September 2010

[3] J Yu, X Zhou, MF Huang, D Qian, PN Ji, "400Gb/s (4× 100Gb/s) orthogonal PDM-RZ-QPSK DWDM Signal Transmission over 1040km SMF-28," Optics Express, vol. 17, no. 20, pp. 17928-17933, 2009.

[4] X. Liu, S. Chandrasekhar, B. Zhu, A.H. Gnauck, and D. W. Peckham, "Transmission of a 448-Gb/s reduced-guard-interval CO-OFDM signal with a 60-GHz optical bandwidth over 2000 km of ULAF and five 80-GHz-Grid ROADMs," Proc. OFC-NFOEC, San Diego, CA, PDPC2, March, 2010.

[5] M. Faruk, Y. Mori, C. Zhang, and K. Kikuchi, "Proper polarization demultiplexing in coherent optical receiver using constant modulus algorithm with training mode," OptoeElectronics and Communications Conference (OECC 2010), pp. 768–769, 2010.

[6] X. Xie, F. Yaman, X. Zhou, and G. Li., "Polarization demultiplexing by independent component analysis," Photonics Technology Letters, IEEE, vol. 22, no. 11, pp. 805-807, 2010.

[7] X. Yao and L. Yan., "Polarization management for polarization division-multiplexing and coherent detection systems," IEEE/LEOS Summer Topical Meetings, pp. 147-148, 2008.

[8] B. Li, K. Larsen, D. Zibar, and I. Monroy, "Over 10 dB net coding gain based on 20% overhead hard decision forward error correction in 100G optical communication systems," Optical Communication (ECOC), 37th on European Conference and Exhibition, pp. 1-3, September 2011.

[9] H. Takahashi, K. Takeshima, I. Morita, and H. Tanaka, "400-Gbit/s Optical OFDM Transmission over 80 km in 50-GHz Frequency Grid," Tu.3.C.1, ECOC 2010.

[10] X. Zhou, L. E. Nelson, P. Magill, R. Issac, B. Zhu, D. W. Peckham, P. Borel, and K. Carlson, "8×450-Gb/s, 50-GHz-spaced, PDM-32QAM transmission over 400km and one 50GHz-grid ROADM," in Proc. OFC-NFOEC 2011, Los Angeles, CA, paper PDPB3, March 2011.

[11] X. Zhou, L. E. Nelson, P. Magill, R. Issac, B. Zhu, D. W. Peckham, P. Borel, and K. Carlson, "800km transmission of 5×450-Gb/s PDM-32QAM on the 50GHz grid using electrical and optical spectral shaping ," accepted for presentation at ECOC 2011, Geneva, Switzerland, paper We.8.B.2, September 2011.

[12] X. Zhou, J. Yu, M. F. Huang, Y. Shao, T. Wang, L. Nelson, P. D. Magill1, M. Birk, P. I. Borel, D. W. Peckham and R. Lingle, "64-Tb/s, 8 b/s/Hz, PDM-36QAM transmission over 320 km using both pre- and

post-transmission digital signal processing," J. Lightwave Technol., vol. 29, no. 4, pp. 571-577, February 15, 2011.

[13] X. Zhou, "An improved feed-forward carrier recovery algorithm for coherent receiver with M-QAM modulation format," IEEE Photonics Technol. Lett., Vol. 22, pp. 1051-1053, 2010.

[14] T. Pfau, S. Hoffmann, and R. Noé, "Hardware-efficient coherent digital receiver concept with feed-forward carrier recovery for M-QAM constellations," J. Lightwave. Technol., vol. 27, no. 8, pp. 989-999, April 15, 2009.

[15] Seb J. Savory, "Digital filters for coherent optical receivers," Optics Express, vol. 16, no. 2, pp. 804-817, 2008.

[16] F. Gardner, "A BPSK-QPSK timing-error detector for sampled receivers," IEEE Transactions on Communications, vol. 34, no. 5, pp. 423-429, 1986.

[17] K. Kikuchi, "Polarization de-multiplexing algorithm in the digital coherent receiver," IEEE/LEOS Summer Topical Meetings, pp. 101-102, 2008.

[18] L. Liu, Z. Tao, W. Yan, S.Oda, T. Hoshida, and J. C. Rasmussen, "Initial tap setup of constant modulus algorithm for polarization de-multiplexing in optical coherent receivers," Proc.of IEEE Optical Fiber Communication, pp. 1-3, 2009.

[19] J. H. Lee and M. H. Sunwoo. "High-speed and low complexity carrier recovery for DP-QPSK transmission," IEEE International Symposium on Circuits and Systems (ISCAS), pp. 438-441, 2011.